# Machine Learning-Based Stroke Segmentation in Kayaking Using Integrated IMU and EMG Data

Gábor Nagy<sup>1</sup>, Péter Katona<sup>2</sup>, Levente Gannorouwa<sup>2</sup> and László Grand<sup>1</sup>

<sup>1</sup>Pázmány Péter Catholic University, Faculty of Information Technology and Bionics, 40 Práter Str, Budapest, Hungary

<sup>2</sup>Hungarian University of Sports Science, 42-48 Alkotás Str, Budapest, Hungary

Keywords: Kayaking, Electromyography, Inertial Measurement Unit, Boat Acceleration, Machine Learning Models,

Ensemble Learning.

Abstract: Accurate classification of stroke side in rowing motions is essential for performance monitoring and injury

prevention. This study evaluates three machine learning models — Naive Bayes (NB), Logistic Regression (LR), and Gradient Boosting Decision Trees (GBDT) — using biomechanical and electromyographic (EMG) features. A core set of 25 features was identified, with normalized joint coordinates and latissimus dorsi EMG activity among the most influential. The NB model achieved 92.21% cross-validation accuracy using only three coordinate-based features, while the full feature set improved accuracy modestly by 1.94%. The LR model attained 94.48% accuracy, slightly outperforming NB. The GBDT model achieved the highest accuracy with 96.18% on the test set, alongside the lowest mean absolute stroke onset detection error of 24.6 ± 51.6 ms, corresponding to just 4.5% of average stroke duration. Classification accuracy remained stable across stroke paces. A strong negative correlation (R = -0.935) between classification accuracy and onset detection error was observed across subjects, indicating that poorer spatial classification corresponds with greater temporal imprecision. Significant inter-subject variability was found, with accuracy ranging from 91.89% to 98.9%, likely reflecting individual differences in stroke technique and muscle activation patterns. A core set of biomechanical features were identified, such as normalized joint coordinates of the ulnar styloid and right olecranon, latissimus dorsi EMG activity among the most influential, vertical pelvis lateral bending and bilateral shoulder flexion. Tempo-based relative time averages of these features reveal clear phase-dependent patterns that contribute strongly to model decision-making. These results demonstrate that accurate stroke side classification can be achieved using a relatively small set of biomechanical features, with GBDT models

## 1 INTRODUCTION

Measuring kayaking technique is inherently complex, requiring the integration of biomechanical, kinematic, and neuromuscular analyses. Recent advancements have expanded the use of technologies such as motion capture systems, surface electromyography (sEMG), and machine learning (ML) models to assess performance more accurately. Kinematic analysis helps quantify joint and segment movement, while sEMG offers insight into muscle coordination and fatigue during paddling, particularly in key upper-body muscles such as the latissimus dorsi, triceps brachii, and anterior deltoid (Lauder and Kemecsey, 1999).

providing superior performance.

Studies such as Garnier et al. have demonstrated that combining sEMG with kinematic data allows for a more complete understanding of how fatigue impacts paddling performance (Garnier et al., 2023). Similarly, McDonnell et al. proposed refined stroke models to address inconsistencies in stroke descriptions, further enhanced by tools like the e-Kayak system for performance feedback (McDonnell et al., 2012; Bonaiuto et al., 2020). Other research has emphasized the value of three-dimensional analyses and recognized inherent movement asymmetries in kayaking that affect force transmission and efficiency (Li, 2017; Vasiljev et al., 2024).

Importantly, multiple studies have reported significant differences between on-water and ergometer-based kinematics. Klitgard et al. found variations in joint movement and increased thoracolumbar motion during on-water trials, while Harbour et al. identified large discrepancies in timing and force parameters across environments (Klitgaard et al., 2021; Harbour

et al., 2021). These findings suggest that ergometerbased assessments may not fully capture the biomechanical realities of on-water performance.

Despite the widespread use of sEMG and motion tracking, our review identified a lack of studies that combine these modalities in on-water kayaking scenarios. This represents a key research gap in understanding how muscle activation and movement interact under real-world conditions.

In parallel, the application of machine learning in sports biomechanics has rapidly progressed. IMU-based data capture combined with ML models has shown strong potential in real-time movement classification, including in kayaking (Kranzinger et al., 2023; Liu et al., 2021). For example, Liu et al. achieved 98% accuracy in segmenting kayak stroke phases using ML validated against video analysis. Similar methodologies have also been successfully applied to gesture recognition tasks using sEMG data, despite challenges such as electrode shift (Kim et al., 2021).

In this study, we investigate whether sEMG and motion capture data can be used to develop an accurate ML model to classify left and right kayak strokes. We also examine the role of input features and explore between-subject variability in classification accuracy. Our hypothesis is that some athletes exhibit more consistent and repeatable stroke patterns, leading to higher classification accuracy, while others display more variation, resulting in reduced model performance. Since classification models perform best with well-separated and consistent input patterns, this work aims to better understand how stroke consistency affects model outcomes and which features are most influential in side prediction and also provide a basis for further analysis.

### 2 METHODS

## 2.1 Participants and Environment

The study involved nine male participants, aged 17 to 21, all of whom were experienced kayakers with notable athletic achievements in the sport. The experiments were conducted over two consecutive days at the Kolonics György Watersport Center, located on the Danube River. These trials took place during mid-summer, under favorable weather conditions. It is noteworthy that the section of the Danube River where the study was conducted is regulated by the Kvassay Dam, which ensures modest presence of natural water currents in the area.

### 2.2 Motion Capture System

A wireless inertial motion capture system (Xsens MVN Link, Xsens Technologies BV, Enschede, Netherlands) and its software (Xsens MVN Studio version 4.2.4, Xsens Technologies BV, Enschede, Netherlands) was utilized to record on water kayaker motion at a sampling rate of 60 Hz. The measurement system consists of small (47 × 30 × 13 mm, 16 g) box shaped measurement units that are placed on both shoulders, upper arms, forearms, hands, thighs, shanks and feet, with one additional sensor placed on the head, chest and on the sacrum of the athlete with Velcro straps.

The measurement units communicate with a base station called Awinda, that are on a boat 5-20 meters away from the athlete. The technology provider claims 50 meter open air wireless range, however in our studies it was significantly less than that, which resulted in signal loss. For better reception a bigger antenna was used in the base station, that somewhat improved signal stability.

Before each recording session a strict IMU unit calibration procedure provided by the manufacturer was strictly followed to avoid electromagnetic fields.

The inertial motion capture systems' data fusion algorithm employed an extended Kalman filter to provide accurate positional readings of body segments and joint angles. In this study we use features from the positional coordinates and joint angles. The XSense biomechanical model consists of 23 segments linked through 22 joints. (Technologies, 2025)

### 2.3 EMG Signal Acquisition

Cometa Miniwave wireless sensors with a WavePlus base station were used to acquire EMG signals and was also used as the boat and paddle accelerometers. The manufacturer claims 40 meters of indoor range. Tested in an outside environment, it is notable that the basestaion was far more reliable than the IMU measurement base station in terms of signal acquisition. Sensors are able to collect EMG data at 2 kHz and also employ an accelerometer that is capable to transfer 3-axis accelerometer data at a sampling rate of 140 Hz

During the exercise sessions, surface electromyography (EMG) signals were collected from various muscles on both the right (abbreviated as "R") and left (abbreviated as "L") sides of the participants. In total 14 sensors were used to collect data from the following specific muscles:

- 1. Latissimus dorsi
- 2. Trapezius (middle fibers)

- 3. Deltoideus Anterior (anterior deltoids)
- 4. Pectoralis Major
- 5. Obliquus Externus Abdominis
- 6. Rectus Femoris
- 7. Flexor Carpi Radialis

These muscles were strategically chosen to capture a comprehensive representation of the muscular activity involved in the kayaking exercise.

In accordance with the international protocol recommendations established by SENIAM (Surface EMG for Non-Invasive Assessment of Muscles), we positioned the surface electrodes on the muscles, specifically targeting the area between the tendon and the motor point. This standardized placement aimed to ensure consistency and reliability in capturing electromyographic signals, facilitating accurate assessment of muscle activity during the kayaking motions under investigation. Adhering to SENIAM guidelines enhances the comparability of our findings with broader scientific literature and contributes to the overall validity of our electromyographic analyses. (Stegeman and Hermens, 2007)

The boat-mounted accelerometer was positioned directly behind the kayaker, aligned with the longitudinal axis of the kayak. From this setup, we utilized acceleration data from the axis parallel to the boat's heading to capture forward motion dynamics. Similarly, the paddle accelerometer was mounted at the midpoint of the paddle shaft, with the relevant axis also aligned parallel to the paddle. This configuration enabled consistent detection of stroke direction and intensity. The parallel axis readings from both devices were essential for accurately deriving stroke side and synchronizing movement phases.

Both the Awinda and WavePlus base stations support hardware synchronization, which we used during the recording process. This hardware sync ensured that both systems began recording at the same time, with their internal clocks aligned. As a result, the timestamps recorded by each system were already synchronized when saved to the computer, enabling accurate temporal alignment of data across devices. The recording was initiated via the WavePlus data acquisition software, which triggered the start of data collection in Xsens as well.

### 2.4 Protocol

Participants were instructed to paddle at a fixed stroke rate for multiple, short, sustainable recording sessions. Stroke rates began at 80 strokes per minute (SPM), representing a low-to-intermediate training load, and increased with 10 SPM incrementally up to 120 SPM, which is considered highly demanding for the athletes. The duration of each recording session was adjusted based on the target stroke rate, allowing for the collection of approximately 60 stroke cycles per session. Specifically, the session lasted 45 seconds at 80 SPM, 40 seconds at 90 and 100 SPM, 35 seconds at 110 SPM, and 30 seconds at 120 SPM. Notably, the 30-second duration at 120 SPM was physically demanding for some athletes, given the high intensity of the effort. A rest period of 60 to 120 seconds was provided between recording sessions to allow for adequate recovery. The protocol ensured that we can gather samples from low-intermediate training scenarios to very demanding intensities. Some athletes performed two runs successively.

An on-land reference trial was conducted to determine the maximum EMG values required for subsequent signal normalization. During this trial, the athlete was instructed to apply maximal force to the kayak paddle while it was held stationary by a helper. This was performed separately for the left and right arms, resulting in isometric contractions that engaged the relevant muscle groups. The resulting EMG maxima provided a consistent and reproducible reference point for normalizing muscle activity recorded during the on-water paddling sessions.

## 3 SIGNAL PROCESSING

## 3.1 IMU Readings

All IMU-derived body segment positions were exported in C3D format for further analysis. Due to the absence of a fixed track, the kayak could not maintain a perfectly straight trajectory during recordings. As a result, the heading and tilt of the athletes were normalized to account for variations in orientation. The center of the pelvis was defined as the origin, and all positional data were translated accordingly.

Motion capture systems are inherently subject to positional drift, a phenomenon that is further amplified in on-water conditions due to the kayak's continuously shifting heading. To mitigate this drift, the biomechanical model was dynamically rotated. Specifically, the model was aligned such that the vector connecting the midpoint between the athlete's heels and the midpoint between the ischial tuberosities (sit bones) was made parallel to the kayak's heading, which in this context is considered the X-axis of the coordinate system. The Z-axis was defined as pointing upward, and the Y-axis pointed leftward relative to the athlete. The biomechanical model of the athlete was rotated within the XY plane such that the

line connecting the seventh cervical vertebra (C7) and the midpoint of the ischial tuberosities was aligned parallel to the Y-axis.

To account for inter-individual differences in body dimensions, per-athlete z-score standardization was applied to the body part coordinate data. These standardized coordinates were then used as features in the subsequent analysis, ensuring comparability across athletes. Joint angles were also normalized on a per-athlete base with z-score standardization.

## 3.2 EMG, Boat and Paddle Accelerometer Preprocessing

To enhance EMG signal quality and minimize the impact of various artifacts, a series of standard preprocessing techniques were applied. A bandpass filter was implemented with cutoff frequencies set at 20 Hz (low) and 400 Hz (high) to remove movement artifacts and high-frequency electrical noise, respectively. The filter was designed as a second-order Butterworth filter to retain the physiologically relevant frequency content of the EMG signals (Raez et al., 2006).

Following filtering, full-wave rectification was performed using a centered moving window of 100 ms. The rectified signal was then smoothed using a Savitzky–Golay filter (window size: 100 ms; polynomial order: 1) to further enhance signal clarity while preserving temporal features.

Finally, all EMG signals were normalized to the maximum EMG amplitude recorded during each athlete's respective on-land reference trial. This normalization allowed for inter-participant comparisons and reduced variability due to individual differences in signal amplitude.

Both boat and paddle accelerometer readings in all axes were preprocessed and smoothed with a Savitzky–Golay filter (window size: 50 ms, polynomial order: 2). High frequency noise does not interfere with resulting measurements.

To ensure uniformity across recordings and facilitate subsequent analysis, all sensor data were resampled to a standardized frequency of 1 kHz. This resampling was carried out using linear interpolation, which estimates intermediate data points to produce evenly spaced time series, thereby allowing consistent comparison and processing across all runs.

## 3.3 Outlier Filtering

Outlier strokes were removed from the analysis using the interquartile range (IQR) method applied to several key stroke metrics. A multiplier of 2 was used to define the lower and upper bounds for outlier detection, identifying strokes with values lying outside this range as outliers. The measurements considered included stroke duration (time taken to complete a single stroke), tempo duration (time taken to complete a full left-right stroke cycle), air phase duration, and the durations of the catch, pull, and recovery phases. Out of 1509 recorded strokes across all athlete runs, 125 strokes were identified as outliers and excluded, resulting in 1384 strokes retained for analysis.

### 4 MODELING

## 4.1 Target Variable

The target variable was computed using synchronized data from both the boat and paddle accelerometers. Stroke segmentation was performed using the boat accelerometer's x-axis — aligned with the kayak's heading — by identifying zero-crossings in the forward acceleration signal, which marked the beginning of new stroke segments. To determine stroke side, we used the paddle accelerometer axis that was parallel to the paddle shaft. For each segmented stroke, we calculated the mean acceleration along this axis. Based on the measurement orientation, strokes with negative mean acceleration values were labeled as left-handed, while those with positive values were labeled as right-handed.

## **4.2** Training and Test Dataset Preparation

A total of 74 runs were collected from nine athletes across varying intensities. Of these, 44 runs were used for model training, feature selection, and parameter optimization, while the remaining 30 runs were reserved for final testing. Each subset maintained a representative distribution of stroke paces, ranging from 80 to 120 strokes per minute, ensuring consistent proportions across all pace classes. Additionally, data from all athletes were included in both training and testing sets to preserve subject diversity. This balanced sampling approach ensured that model evaluation reflected a comprehensive range of performance conditions

We employed a 6-fold grouped cross-validation across 18 available training runs. Grouping ensured that all samples from the same run (i.e., from the same subject and session) remained entirely within either the training, validation or test set for each fold, thereby preventing data leakage. This approach is

particularly appropriate when dealing with repeated measures or correlated observations — such as multiple recordings from the same athlete — as it reduces the risk of overfitting to individual-specific patterns. Furthermore, non-overlapping runs of varied intensities were selected to enhance independence between training and validation subsets, improving generalization to unseen conditions.

We have chosen accuracy as the error metric for all because of interpretability. We also employed the error metric mean absolute stroke on-set difference (MAEOSD): that is the mean absolute difference measured in samples between the true onset of a successive stroke and the predicted onset of the stroke.

#### 4.3 Models

We compare results of 3 classifiers: Gaussian Naive Bayes, Logistic Regression, Gradient Boosting Decision Tree.

Gaussian Naive Bayes (NB) is a probabilistic classifier based on Bayes' Theorem, assuming independence between features and that they follow a normal (Gaussian) distribution. It is simple, fast, and works well with small datasets or when the independence assumption roughly holds.

Logistic Regression (LR) is a linear model used for binary classification, which estimates the probability of a class label using the logistic (sigmoid) function. It assumes a linear relationship between input features and the log-odds of the outcome, and it's effective for well-separated classes with linearly separable boundaries.

Gradient Boosting Decision Trees (GBDT) is an ensemble method that builds a series of decision trees sequentially, where each new tree corrects errors made by the previous ones. It combines the strengths of multiple weak learners to produce a strong classifier, often achieving high accuracy on complex, nonlinear datasets. GBDT is more computationally intensive but generally offers superior performance compared to simpler models. (Chen and Guestrin, 2016)

A Gaussian Naive Bayes classifier was employed as a baseline to benchmark the performance of more complex models. Performance metrics are reported as the average classification accuracy across six cross-validation folds and on the held-out test set.

The classifiers operated on a per-sample basis, assigning a confidence score to each time point, indicating the likelihood of it corresponding to a left or right-hand stroke. Training was also conducted at the persample level, enabling the model to learn fine-grained temporal patterns specific to stroke side. Accordingly, the accuracy metric can be interpreted as the propor-

tion of time during which the classifier correctly identified the stroke side.

#### **4.4** Feature Selection

To reduce dimensionality and improve performance feature selection techniques were implemented: for Naive Bayes and Logistic Regression forward selection and backward elimination were both used. These stepwise feature selection techniques commonly used in machine learning. Forward selection begins with an empty model and iteratively adds the feature that improves the error metric (accuracy in this case). In contrast, backward elimination starts with the full set of features and progressively removes the least significant ones, continuing until no further improvement in model performance is observed. We used backward elimination on the feature set obtained with forward selection to reduce the feature space. Once no further improvement was observed, Greedy Backward Elimination was applied to remove any features whose exclusion resulted in improved accuracy. This process of forward selection followed by backward elimination continued iteratively until no additional modifications improved model performance.

## 4.5 Feature Importance

Following feature selection, permutation importance was employed to further evaluate and interpret feature contributions. This model-agnostic technique estimates feature importance by randomly permuting feature values and measuring the resulting drop in performance. Features causing greater reductions in accuracy were deemed more important. This provided a robust and interpretable measure of feature relevance, especially beneficial for understanding complex or non-linear models, but also helps with simple models that do not provide an intrinsic feature importance such as Naive Bayes. Features with negative permutation importance scores were discarded.

### 5 RESULTS

## 5.1 Naive Bayes

The final selected feature set contained 25 features and achieved a cross-validation accuracy of 94.71%  $\pm$  0.01 and 94.48% on the test set. Among all features, the most influential were the normalized Z-coordinates of the left olecranon and both left and right ulnar styloid markers. Remarkably, using just these three features, the Naive Bayes classifier

achieved 92.21% accuracy in cross-validation. The additional 23 features contributed a modest 2.5% improvement, suggesting that the model performs effectively even with a very minimal feature set. This finding has practical implications for applications where data collection capabilities are limited. This finding shows that using only joint coordinates would be sufficient to classify stroke sides.

### 5.2 Logistic Regression

The final model contained 28 features the validation set accuracy was  $94.38\% \pm 0.005$ , slightly worse than the NB classifier and achieved 94.53% on the test set. The model used features from all three feature sets. The final model parameters used were L2-penalty, C=100.0 (inverse of regularization strength, smaller values specify stronger regularization). Interestingly the top-5 most important features would produce a  $93.46\% \pm 0.01$  accuracy, and the top-3 would only achieve  $88.72\% \pm 0.02$ . The top 5 features include T8-right upper arm lateral bending and vertical pelvis axial bending, along with normalized EMG readings of the latissimus dorsi and the right olecranon Z-coordinate.

## 5.3 Gradient Boosting Decision Tree

We first trained a base model of GBDT with all features and selected the top-50 most important features, after that we gradually decreased the number of features until accuracy improved. The final model used 33 features. After hyperparameter tuning, the best validation accuracy was achieved with: 15 leaves, a learning rate of 0.050, colsample = 0.75, and subsample = 0.50. The best model achieved  $96.02\% \pm 0.01$  on the validation set and 96.18% on the test set. The top-5 most important features produce a model with  $94.83\% \pm 0.01$  accuracy. The used features are left ulnar stiloid Z-coordinate and right top of hand Z-coordinate, with left and right latissimus dorsi and left shoulder abduction adduction joint angles.

### **5.4** Feature Importances

A core set of features (Figure 1) was identified as important across all three models, including the normalized left ulnar styloid Z coordinate, right olecranon Z coordinate, bilateral latissimus dorsi EMG activity, vertical pelvis axial bending, left flexor carpi radialis EMG activity, bilateral shoulder flexion/extension, and bilateral knee abduction/adduction. When expanding the analysis to features selected by at least two models, additional relevant variables include

T8-right upper arm lateral bending, right ulnar styloid (particularly important for the Naive Bayes model), and left shoulder abduction/adduction, along with several lower-importance features. Notably, in the best-performing GBDT model, the right top of hand Z coordinate had high relative importance, despite not being selected by the other models.

The identified feature set reveals a clear anatomical and functional grouping relevant to kayaking performance. Upper limb features, including wrist and elbow positions, shoulder joint angles, and upperbody EMG activity, contribute primarily to paddle control and propulsion. Trunk features, such as vertical pelvis axial bending and upper spinal lateral bending, reflect core stability and rotational control during the stroke. Lower limb features, notably knee abduction/adduction, indicate the role of leg positioning in anchoring and force transfer. These findings highlight the interdependence of upper body mechanics, trunk stability, and lower limb engagement in accurately distinguishing stroke sides using machine learning models.



Figure 1: List of most important features by model.

In terms of feature utilization, both NB and LR models rely on a smaller but more discriminative feature set, while GBDT makes use of a broader range of features—likely due to its use of random resampling during training. Interestingly, the NB model showed strong performance using only coordinate-based features, suggesting that, in resource-constrained scenarios, coordinate data alone may suffice for side classification. GBDT achieved the highest overall accuracy, benefiting from its ability to model feature interactions, though this advantage resulted in only a 2.5% improvement. While NB slightly outperformed LR in the validation set and underperformed it in the test set, the marginal accuracy gain does not justify its higher complexity.

Tempo-based relative time averages — calculated across all available data (training and test sets combined) — are shown in Figure 2 for the five most important features: normalized left ulnar styloid Z coor-

dinate, right olecranon Z coordinate, bilateral latissimus dorsi EMG activity, and vertical pelvis axial bending. The blue vertical line indicates the midpoint of the tempo, separating right and left hand strokes. These features consistently ranked highest in importance across all classifiers, reflecting their reliability and discriminative power for stroke side classification.

The temporal profiles of these features reveal distinct and interpretable biomechanical patterns. For example, the bilateral latissimus dorsi muscles show unilateral activation that aligns with the stroke side, being active only during the corresponding stroke phase. Shoulder flexion/extension patterns also show a clear alternation across the tempo midpoint, with the left shoulder exhibiting positive values during righthand strokes and negative values during left-hand strokes. Notably, the normalized Z coordinates of the left ulnar styloid and right olecranon cross over at the stroke transition. The right olecranon Z coordinate remains below 0.25 during right strokes and rises above 0.25 during left strokes, while the left ulnar styloid shows the inverse pattern. These coordinated shifts across features illustrate a synchronized change in posture and muscle engagement, reinforcing their significance in stroke classification. These profiles may be used as templates for stroke separation and to identify systematic errors in athletes.

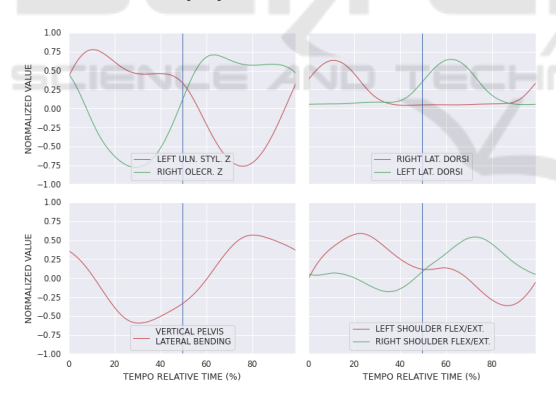


Figure 2: Tempo relative time feature averages.

### 5.5 Statistical Analysis of Errors

Model performances are summarized in Table 1. To evaluate the differences in classification accuracy among the three models—Logistic Regression (LR), Naive Bayes (NB), and Gradient Boosting Decision Trees (GBDT)—we conducted statistical tests on the cross-validation results. Normality of the pairwise differences in model accuracies was assessed using the Shapiro-Wilk test. The results indicated no significant deviation from normality for any model pair:

LR vs. NB (W=0.922, p=0.543), NB vs. GBDT (W=0.899, p=0.404), and LR vs. GBDT (W=0.999, p=0.9998). These results justify the use of parametric tests for further comparisons.

Three paired-sample t-tests were performed to compare model accuracies. There was no statistically significant difference between LR and NB (t=-0.964, p=0.390). However, GBDT showed significantly higher accuracy compared to both LR (t=13.816, p=0.0001) and NB (t=7.564, p=0.0016). These findings suggest that GBDT outperforms both LR and NB in classification accuracy under the tested conditions.

Table 1: Stroke side classification accuracy of machine learning models on validation and test set (%).

	Accuracy	
Model	Val. set	Test set
NB	94.71	94.48
LR	94.38	94.53
GBDT	96.02	96.18

Table 2 summarizes the MAEOSD of the classifiers in milliseconds. As expected, the GBDT model achieved the best performance, with a mean absolute onset difference of  $24.6 \pm 51.6$  ms. Considering that the average stroke duration in the test set is 639.6  $\pm$  88.4 ms, this corresponds to an average onset detection error of only 4.5%, highlighting the GBDT model's suitability for real-time classification scenarios. The results show that the GBDT model achieves tolerable stroke onset duration error.

Table 2: Mean absolute onset differences on the test set (ms).

Model	MAEOSD
NB	$36.5 \pm 56.4$
LR	$35.5 \pm 49.7$
GBDT	$24.6 \pm 51.6$

Per-sample predictions were also aggregated at the stroke level to evaluate whether any entire strokes were misclassified. On the validation set, 14 misclassified strokes were observed for both the NB and LR models, while the GBDT model misclassified 12 strokes. Notably, no misclassified strokes were found in the test set for any of the models. These results indicate that all three models achieve high aggregate accuracy at the stroke level.

Figure 3 illustrates the classification accuracy of left and right hand strokes across the normalized stroke cycle for the GBDT model. The two curves are nearly identical, indicating symmetrical model performance between stroke sides. As anticipated, classification accuracy declines in the first and last 10%

of the stroke cycle — regions associated with greater motion variability and transitional dynamics. This observation aligns with earlier findings on stroke onset detection error, which is most pronounced at stroke boundaries. In contrast, the central 80% of the stroke is consistently classified with high accuracy, suggesting that mid-stroke movement patterns are more stable and distinguishable.

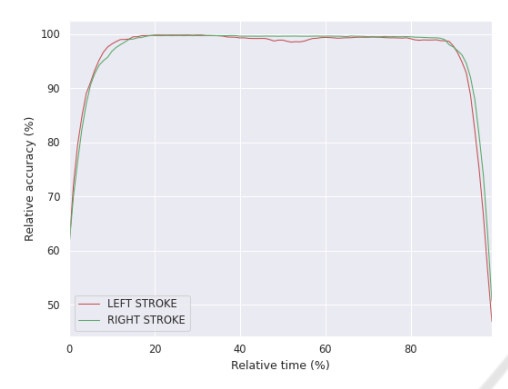


Figure 3: Relative time accuracy for left and right hand strokes of GBDT model.

An increase in stroke pace does not appear to significantly impact the overall classification efficiency of the models. Interestingly, the 90 strokes per minute (SPM) condition yields the highest average stroke onset detection error and the lowest classification accuracy among all tested stroke rates for the best-performing GBDT model. This decrease in accuracy is primarily due to an outlier on-water measurement test that yielded only 88% accuracy. When this outlier is excluded, stroke pace does not have a statistically significant effect on classification accuracy, indicating that the model generalizes well across a range of movement speeds and model performance is stable and robust with respect to variations in stroke frequency.

Figure 4 presents the per-subject classification accuracy (x-axis) plotted against the mean absolute onset detection error (y-axis). A very strong negative correlation is observed between these two metrics (Pearson's R=-0.9346). The fitted regression line has a slope of -8.55, meaning that for every 1% increase in classification accuracy, the mean absolute onset detection error decreases by approximately 8.55 milliseconds. This result suggests that improvements in classification performance are directly associated with greater temporal precision in detecting stroke onset.

In practical terms, subjects for whom the model struggles to correctly classify stroke sides also tend to show larger deviations in onset timing. This highlights the interdependence of spatial and temporal as-

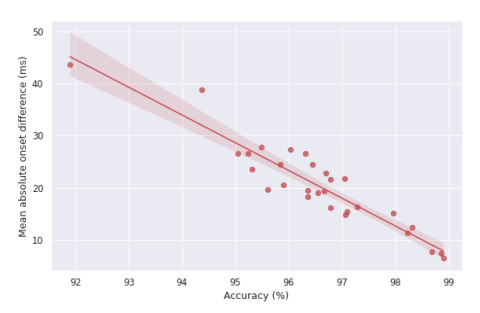


Figure 4: Per-subject accuracy and mean absolute onset difference (outlier removed).

pects of stroke recognition, and suggests that efforts to improve classification accuracy may also yield benefits in onset timing accuracy.

This relationship is further supported by the trends observed in Figure 3, which shows classification accuracy across the normalized time course of a stroke. Accuracy is lowest at the earliest (0–10%) and latest (90–100%) segments of a stroke, where motion tends to be more variable and transitions are more subtle. These boundary regions likely contribute disproportionately to onset detection error, reinforcing the connection between reduced accuracy and timing imprecision.

The primary factor affecting classification error appears to be inter-subject variability, with accuracy rates differing significantly between athletes, ranging from 91.89% to 98.9%, when the outlier is removed.

This variability likely reflects individual differences in technique and style concentrated in the transitional period between two strokes, which warrants further investigation in future research.

We hypothesize that subjects exhibiting lower accuracy rates demonstrate greater variability in the features utilized by the GBDT model. Such variability may arise from inconsistent stroke techniques, a wider range of hand movement patterns, or variations in muscle activation timing and intensity, all of which can challenge the model's ability to generalize and accurately classify stroke sides. Conversely, athletes with a more stable and consistent style are likely to produce more homogeneous training data, resulting in higher classification accuracy. Furthermore, we propose that athletes with higher classification accuracy may display a reduced number of distinct muscle activation sequences, potentially due to less variability in technique or lower muscle fatigue. These insights emphasize the importance of individual biomechanical factors in classifier performance and highlight avenues for personalized model optimization.

## 6 CONCLUSION

This study evaluated and compared the performance of three machine learning models — Naive Bayes (NB), Logistic Regression (LR), and Gradient Boosting Decision Trees (GBDT) — for classifying stroke sides based on biomechanical and electromyographic features. A core set of features, primarily normalized joint coordinate data and Latissimus Dorsi EMG activity, was found to be highly informative across all models. Remarkably, the NB classifier achieved strong accuracy using only a minimal feature set consisting of three coordinate-based variables, highlighting its potential utility in scenarios with limited data acquisition capabilities.

Among the models, GBDT demonstrated the highest classification accuracy (96.69% on the test set) and the lowest stroke onset detection error (24.6  $\pm$  51.6 ms), indicating its suitability for real-time applications despite increased model complexity. Logistic Regression offered a modest improvement over NB but with only marginal gains relative to the additional complexity involved. The strong negative correlation between classification accuracy and onset detection error suggests that improvements in spatial classification directly enhance temporal precision.

Stroke pace and side had minimal effect on model performance, whereas significant inter-subject variability was observed. This variability likely reflects individual differences in stroke technique and muscle activation patterns, which influence classifier accuracy. Athletes with more consistent movement patterns exhibited higher accuracy, underscoring the importance of personalized biomechanical factors in model generalization.

Importantly, since the most critical features include joint coordinates, these results suggest that pose estimation models applied to video feeds could provide a practical and non-invasive means of acquiring the necessary data for stroke side classification. This opens the possibility of implementing the classification pipeline in real-world settings without the need for extensive sensor instrumentation.

Finally, we plan to test our hypotheses regarding muscle activation order and per-subject variability in future research to better understand their impact on classification performance and to improve model personalization.

Overall, these findings demonstrate that effective stroke side classification can be achieved using a relatively small set of biomechanical features, with gradient boosting methods providing the best performance. Future work should explore subject-specific adaptations, further investigate biomechanical sources of inter-subject variability, and evaluate the integration of video-based pose estimation for broader applicability.

### REFERENCES

- Bonaiuto, V., Gatta, G., Romagnoli, C., Boatto, P., Lanotte, N., and Annino, G. (2020). A pilot study on the e-kayak system: A wireless daq suited for performance analysis in flatwater sprint kayaks.
- Chen, T. and Guestrin, C. (2016). Xgboost.
- Garnier, Y. M., Hilt, P. M., Sirandre, C., Ballay, Y., Lepers, R., and Paizis, C. (2023). Quantifying paddling kinematics through muscle activation and whole body coordination during maximal sprints of different durations on a kayak ergometer: A pilot study. *International Journal of Environmental Research and Public Health*, 20(3).
- Harbour, E., McAlpine, P., and Neville, J. (2021). Paddle mechanics differ between on-water and ergometer sprint kayaking.
- Kim, J., Koo, B., Nam, Y., and Kim, Y. (2021). semg-based hand posture recognition considering electrode shift, feature vectors, and posture groups.
- Klitgaard, K. K., Hauge, C., Oliveira, A. S., and Heinen, F. (2021). A kinematic comparison of on-ergometer and on-water kayaking. *European Journal of Sport Science*, 21(10):1375–1384. PMID: 33001757.
- Kranzinger, C., Bernhart, S., Kremser, W., Venek, V., Rieser, H., Mayr, S., and Kranzinger, S. (2023). Classification of human motion data based on inertial measurement units in sports: A scoping review.
- Lauder, M. and Kemecsey, I. (1999). Kayak technique diagnosis and remedies, part two. *Canoe Focus*, pages 18–19
- Li, M. (2017). The progress of biomechanical researches in kayaking.
- Liu, L., Wang, H., Qiu, S., Zhang, Y., and Hao, Z.-D. (2021). Paddle stroke analysis for kayakers using wearable technologies.
- McDonnell, L. K., Hume, P., and Nolte, V. (2012). An observational model for biomechanical assessment of sprint kayaking technique.
- Raez, M. B., Hussain, M. S., and Mohd-Yasin, F. (2006). Techniques of emg signal analysis: detection, processing, classification and applications. *Biological Procedures Online*, 8:11–35. Epub 2006 Mar 23. Erratum in: Biol Proced Online. 2006;8:163. doi: 10.1251/bpo124.
- Stegeman, D. and Hermens, H. (2007). Standards for suface electromyography: The european project surface emg for non-invasive assessment of muscles (seniam). 1.
- Technologies, M. (2025). Xsens biomechanical model.
- Vasiljev, R., Vasiljev, I., Voronin, D. I., and Zhigalina, A. (2024). Features of pressure asymmetry manifestation on the seat of kayakers on a rowing ergometer.